Singlet Oxygen Generation in Classical Fenton Chemistry

Andrew J. Carrier,[‡a] Saher Hamid,[‡a] David Oakley,[a] Ken Oakes,[b] and Xu Zhang[a*]

[a]Verschuren Centre for Sustainability in Energy and the Environment and [b]Department of Biology, Cape Breton University, 1250 Grand Lake Road, Sydney, Nova Scotia, B1P 6L2, Canada.

[*]Corresponding Author. E-mail: Xu_Zhang@cbu.ca
[‡]These authors contributed equally to the work.

The Fenton reaction, the Fe-catalyzed conversion of hydrogen peroxide to reactive oxygen species (ROS) was discovered more than a century ago.[1] It occurs widely in nature because of the ubiquity of Fenton reagents, i.e., Fe and H_2O_2, and ROS in environmental and biological systems;[2] however, its mechanisms and the identity of the ROS generated under varying conditions have remained controversial. The widely accepted mechanism is that of successive oxidation and reduction of Fe^{2+} and Fe^{3+} by hydrogen peroxide to form $^{\cdot}OH$ and $O_2^{\cdot-}$, respectively, where $^{\cdot}OH$ is implicated as the primary oxidant.[3,4] The reaction is commonly performed at low pH where Fe is more reactive, ROS generation rate is high, and the $^{\cdot}OH$ generated have higher oxidizing potential, i.e., higher E^{0}.[5–7] However, the formation of high-valent Fe^{4+}=O species has also been implicated.[8] The controversy persists because of the short lifetimes of these ROS, which renders their direct detection difficult or impossible.

Herein, by systematically dissecting the contributions of various ROS species generated in the classical Fenton reaction by using specific ROS traps and scavengers, we identified that singlet oxygen ($^1O_2$) is the main ROS from pH 4–7. In contrast, although $^{\cdot}OH$ is produced in measurable quantities, it was not a major contributor to the oxidation of organic molecules.

$^1O_2$ formation is supported by the following lines of evidence. First, Singlet Oxygen Sensor Green (SOSG), which selectively forms a fluorescent endoperoxide upon reaction with $^1O_2$,[9] generates a positive signal when exposed to classical Fenton conditions (Fig. 1). Second, under classical Fenton conditions, 1,3-diphenylisobenzofuran (DPIBF) is selectively converted to o-dibenzoylbenzene, which is the product formed after fragmentation of an initial $^1O_2$-endoperoxide adduct (Fig. 2, confirmed via GC-MS).[10,11] Third, the oxidation of a non-selective redox indicator, o-phenylenediamine (OPD), is inhibited in a dose-dependent manner by sodium azide, an established $^1O_2$ scavenger,[12,13] but not by the established $^{\cdot}OH$ scavengers, tert-butyl alcohol[14] and coumarin[15,16] (Fig. 3). Notably, even though we do not see direct evidence for the formation of Fe^{4+}=O, our results do not exclude the formation of an Fe^{4+} intermediate. However, prior work by Pestovsky et al. unambiguously produced Fe^{4+}=O from Fe^{3+} and O_3, confirmed with Mössbauer spectroscopy and X-ray absorption spectroscopy; using such spectroscopy characteristics, formation of Fe^{4+}=O was ruled out in acidic and neutral aqueous solution with Fenton reagents.[17] Wiegand et al. also used kinetic studies to eliminate Fe^{4+} as a significant oxidant species at pH 1–4.[18]

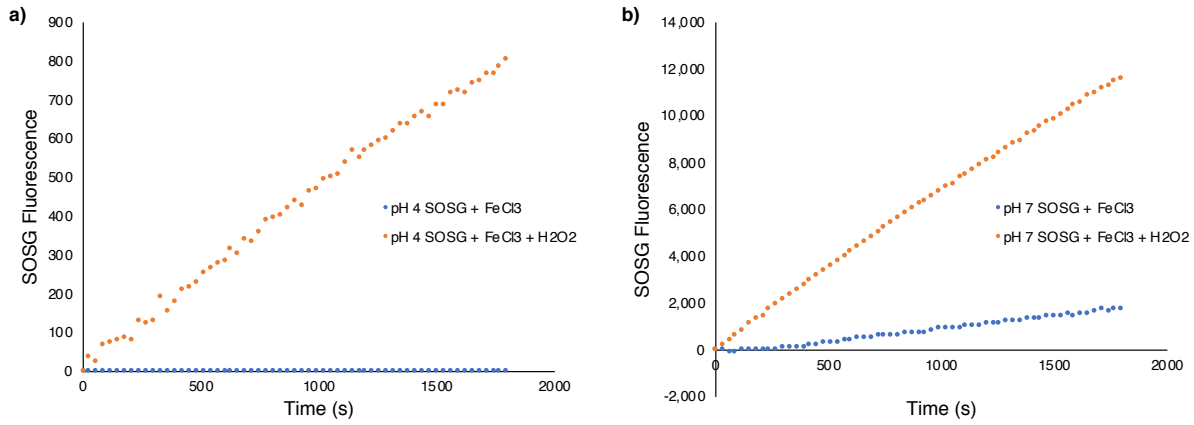

Figure 1. Increasing fluoresence intensity of Singlet Oxygen Sensor Green (SOSG) as a function of time at a) pH 4 and b) pH 7. Note the quenching of fluorescence at low pH. $[SOSG]_0$ = 100 µM; $[FeCl_3]_0$ = 50 µM; $[H_2O_2]$ = 500 mM; [MES] = 1 mM; and T = 25 ºC.

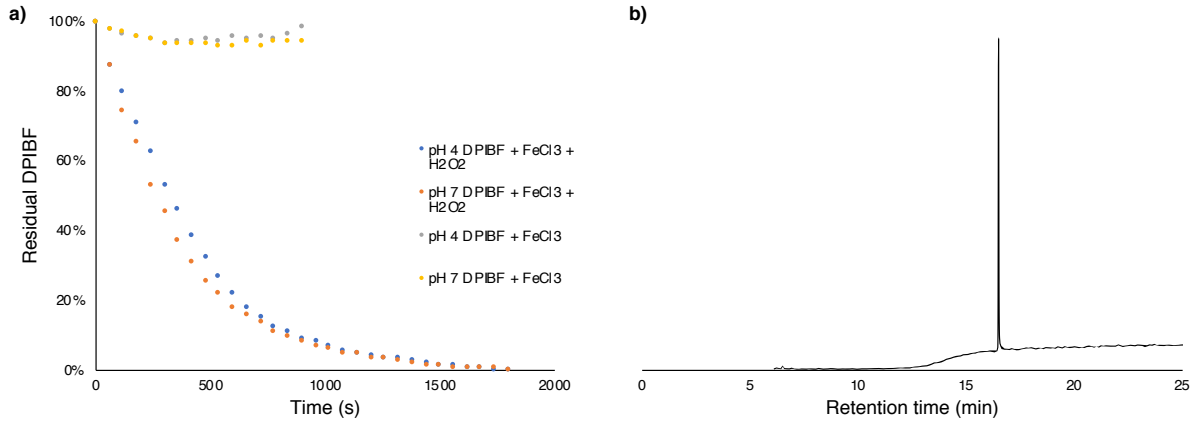

Figure 2. a) Conversion of 1,3-diphenylisobenzofuran (DPIBF) to 1,2-dibenzoylbenzene as a function of time. b) GC-MS chromatogram of the 1,2-dibenzoylbenzene product. $[DPIBF]_0$ = 500 µM; $[FeCl_3]_0$ = 50 µM; $[H_2O_2]_0$ = 200 mM; [MES] = 1 mM; and T = 25 ºC.

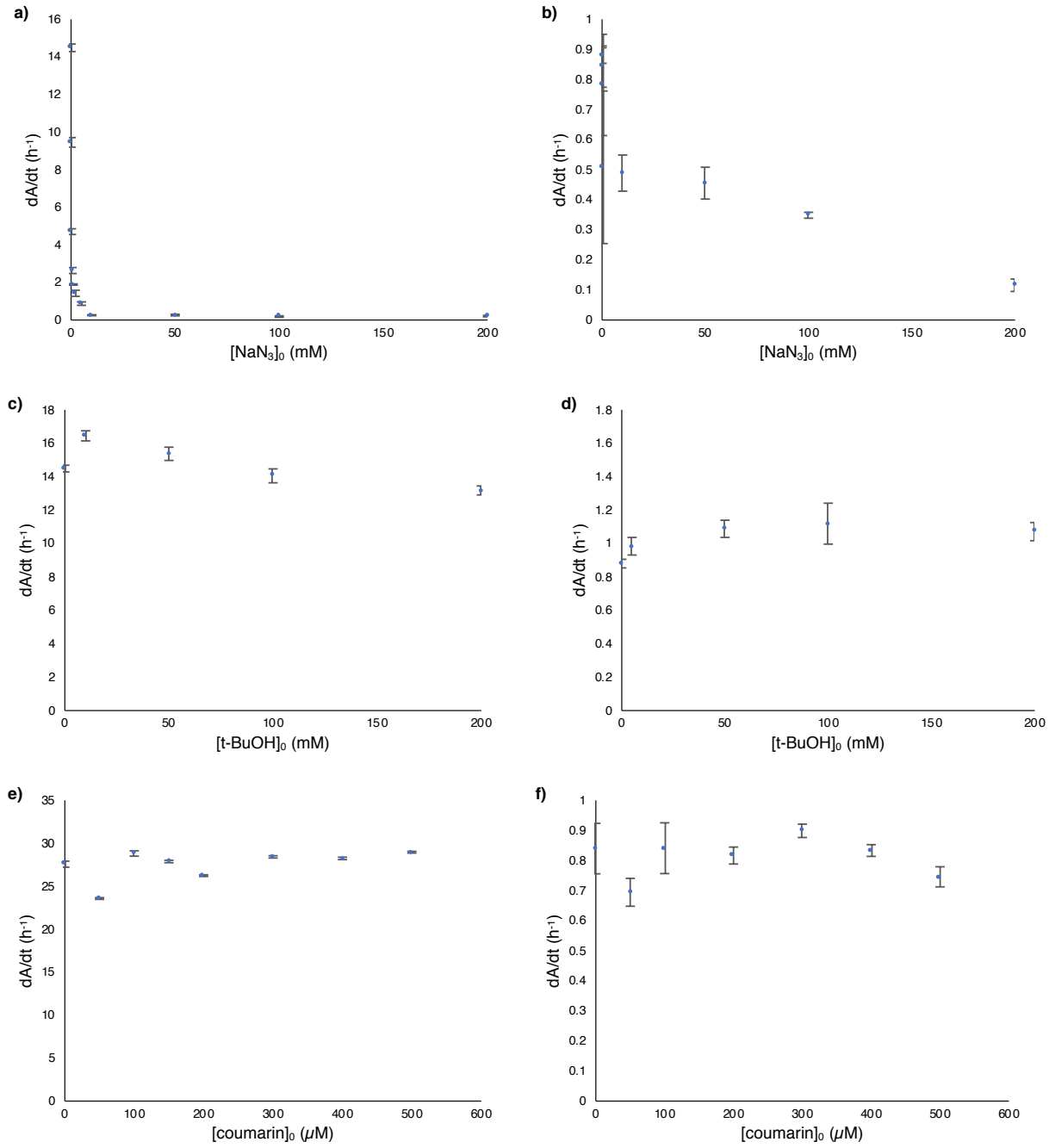

Figure 3. Oxidation of o-phenylenediamine (OPD) in the presence of increasing concentrations of a) and b) sodium azide, c) and d) t-BuOH, and e) and f) coumarin. Panels a), c), and e) were pH 4, while panels b), d), and f) were conducted at pH 7. Sodium azide is a singlet oxygen scavenger and t-BuOH and coumarin are hydroxyl radical scavengers. $[OPD]_0$ = 200 µM, $[FeCl_3]_0$ = 200 µM, $[H_2O_2]_0$ = 200 mM, [MES] = 1 mM, T = 25 ºC.

The conversion of coumarin to umbelliferone supports the formation of $^{\cdot}OH$ over the course of the Fenton reaction (Fig. 4);[15,16] however, as above, quenching the $^{\cdot}OH$ radicals with either coumarin or TBA does not significantly reduce the OPD oxidation (Fig. 3c–f), which is indicative

of the total amount of oxidant generation in the system. This result confirms the minor role of ·OH as the oxidant; nevertheless, ·OH can be either a side product or an intermediate in the formation of the primary oxidant, $^1O_2$.

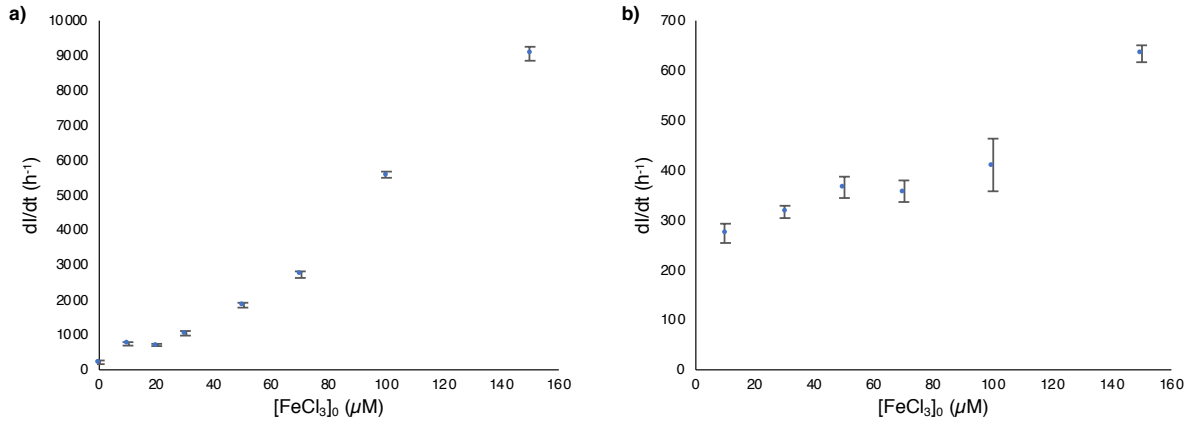

Figure 4. Umbelliferone formation through the hydroxylation of coumarin by hydroxy radicals as a function of $[FeCl_3]_0$ at a) pH 4 and b) pH 7. $[coumarin]_0$ = 100 µM; $[H_2O_2]_0$ = 200 mM; [MES] = 1 mM.

Because the direct precursor for $^1O_2$ formation is likely through the oxidation of $O_2^{\cdot-}$ by Fe^{3+},[19,20] we performed experiments to detect free $O_2^{\cdot-}$ over the course of the Fenton reaction under varying conditions. To achieve this, we used XTT dye (2,3-bis-(2-methoxy-4-nitro-5-sulfophenyl)-2H-tetrazolium-5-carboxanilide, disodium salt) as a colorimetric indicator, which can be reduced by $O_2^{\cdot-}$ to quantitatively generate a colorimetric signal.[21] Notably, significant amounts of $O_2^{\cdot-}$ were detected at neutral and basic pH, where $O_2^{\cdot-}$ is both a stronger reducing agent and may be more readily displaced from the Fe centers by $^-$OH anions, thus facilitating detection (Fig. 5).[22] Under acidic conditions HOO· is a poorer reductant and there are fewer $^-$OH in solution to displace it from the iron ions, and it is thus not easily detectable.[22]

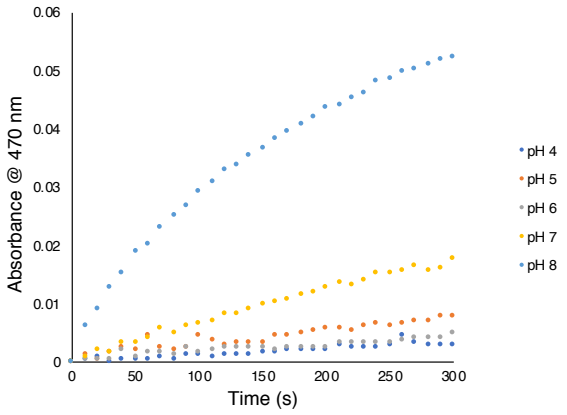

Figure 5. XTT reduction as a function of time with varying pH, indicating the generation of superoxide anions, i.e., $O_2^{\cdot-}$. $[XTT]_0$ = 1 mM; $[FeCl_3]_0$ = 50 µM; $[H_2O_2]$ = 200 mM; [MES] = 1 mM; T = 25 ºC.

We further tested the presence of an Fe^{4+}=O species through electrochemical measurements, without direct evidence for their presence. This is in agreement with prior work that Fe^{4+}=O produced from Fe^{3+} and O_3 rather than in Fenton reaction systems.[17]

Mechanistic interpretation

At each tested pH, the rate of ROS generation (as measured through OPD colorimetric oxidation reaction) is first order in terms of Fe^{3+} and H_2O_2 and independent of Cl^- (Figs. 6–8). Interestingly, the slope of initial rate as a function of $[Fe^{3+}]$ abruptly changes slope at $[Fe^{3+}]$ ~ 214 µM (Fig. 6), which may indicate a change in rate determining step. This is consistent with the mechanism proposed by Moffett and Zika that identifies O_2 (but not $^1O_2$) as the final reaction product (Scheme 1, Equations 1–4).[4]

$$Fe^{2+} + H_2O_2 \rightarrow Fe^{3+} + {}^{\cdot}OH + {}^{-}OH \quad (1)$$
$$Fe^{3+} + H_2O_2 \rightarrow Fe^{2+} + O_2^{\cdot-} + 2H^+ \quad (2)$$
$$Fe^{2+} + {}^{\cdot}OH \rightarrow Fe^{3+} + {}^{-}OH \quad (3)$$
$$Fe^{3+} + O_2^{\cdot-} \rightarrow Fe^{2+} + {}^1O_2 \quad (4)$$

Notably, even though $^1O_2$, rather than $^{\cdot}OH$ radicals, is the main ROS (Fig. 3), the amount of $^{\cdot}OH$ (indicated by coumarin oxidation) and the total amount of ROS (indicated by the OPD oxidation and dominated by $^1O_2$) generated follow the same trends as a function of solution pH, which is dependent on the ligand environment around the iron ions and supports the hypothesis that $^{\cdot}OH$ is an intermediate on $^1O_2$ formation pathway (Fig. 9).[4] However, the detectable superoxide ions $O_2^{\cdot-}$ do not follow this trend, which is understandable, because it can rapidly undergo inner electron transfer to Fe^{3+} without leaving the complex, which appears to be strongly influenced by the ^-OH anion concentration. The presence of ^-OH anions can reduce the solubility of Fe (although these ions remain soluble under our reaction conditions, because our Fe concentrations were low) and changes the redox potential difference of the complex, e.g., the couples $Fe(OH)_2^+/Fe(OH)_2$, $Fe(OH)^{2+}/Fe(OH)^+$, and Fe^{3+}/Fe^{2+} have standard reduction potentials of -0.04, +0.304, and +0.771 V, respectively (additionally $FeCl^{2+}/FeCl^+$ has a standard reduction potential of +0.773 V, explaining the nil effect of added NaCl).[4] Each of these reactions was accelerated as the pH of the solution decreased from 7 to 4 (although there was strong fluorescence quenching of SOSG at low pH values). The reaction is fastest at low pH where Fe^{3+} remains fully soluble with no ^-OH ligands (Figs. 1–5). Changing the solvent from water to D_2O reduced the reaction rate at both pH 4 and 7, indicating proton transfer is occurring during the rate determining step (RDS) of the reaction (either Eq. 1 or 2, with the pH effect supporting Eq. 2); in contrast, the oxidation of OPD by $^1O_2$ was not the RDS, because otherwise the OPD oxidation would be enhanced, as the lifetime of $^1O_2$ in D_2O is ~20 times longer than in H_2O (Fig. 10).[23]

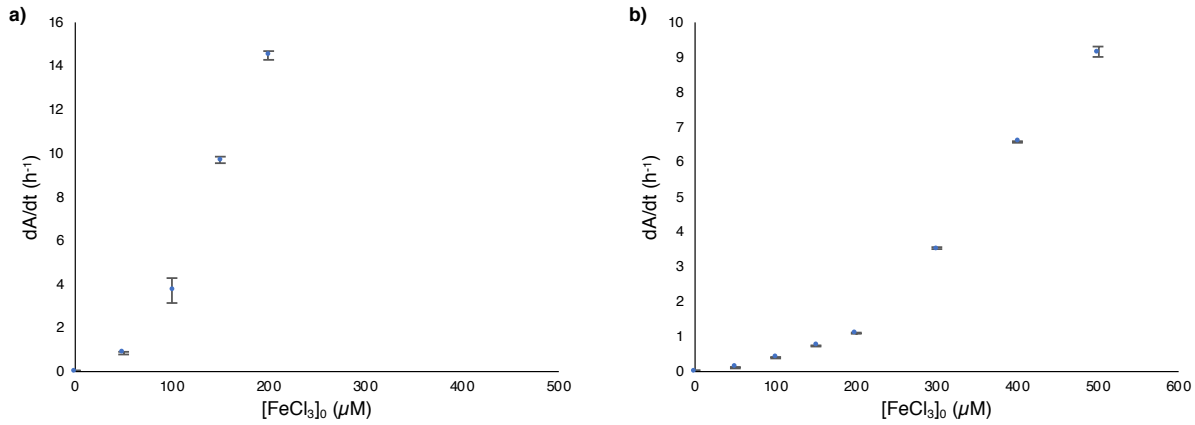

Figure 6. Oxidation of o-phenylenediamine (OPD) as a function of varying $[FeCl_3]_0$ at a) pH 4 and b) pH 7. $[OPD]_0$ = 200 µM; $[H_2O_2]_0$ = 200 mM; [MES] = 1 mM; and T = 25 ºC.

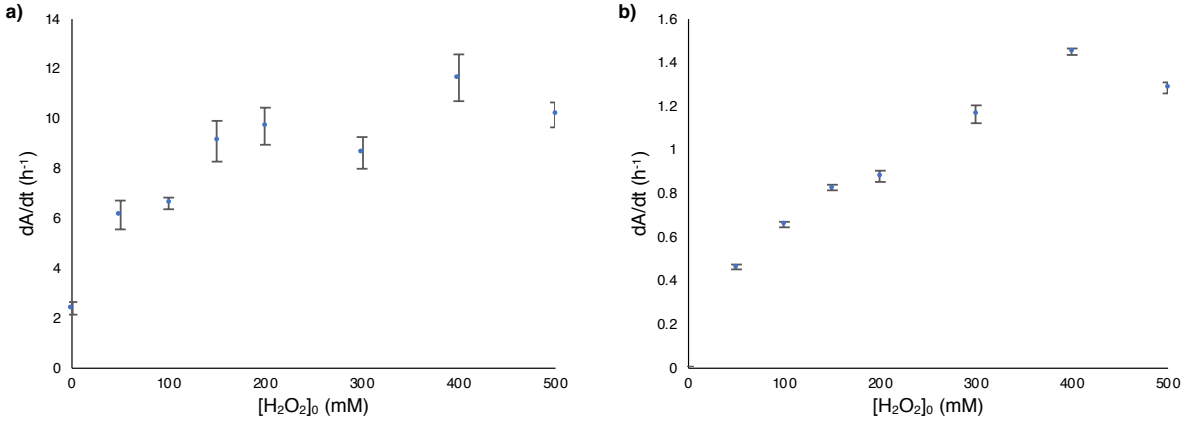

Figure 7. Oxidation of o-phenylenediamine (OPD) as a function of $[H_2O_2]_0$ at a) pH 4 and b) pH 7. $[OPD]_0$ = 200 µM; $[FeCl_3]_0$ = 200 µM; [MES] = 1 mM; and T = 25 ºC.

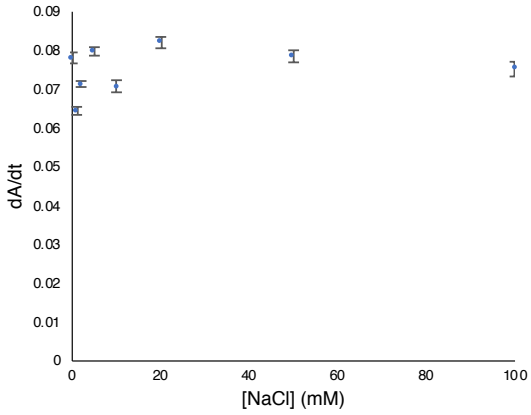

Figure 8. Initial rate of o-phenylenediamine (OPD) oxidation as a function of [NaCl]. $[FeCl_3]_0$ = 500 µM, $[OPD]_0$ = 500 µM, $[H_2O_2]_0$ = 500 mM, [MES] = 1 mM, pH = 7, T = 25 ºC.

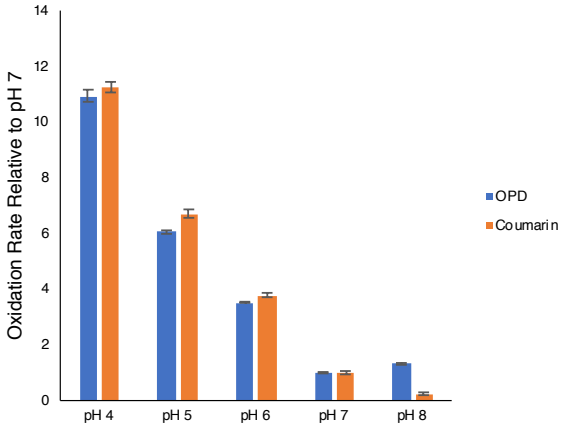

Figure 9. Relative rates of hydroxyl radical (coumarin oxidation) and singlet oxygen generation (OPD oxidation) as a function of pH. $[OPD]_0$ = 200 µM or $[coumarin]_0$ = 100 µM, $[FeCl_3]_0$ = 50 µM, $[H_2O_2]_0$ = 200 mM, [MES] = 1 mM, T = 25 ºC.

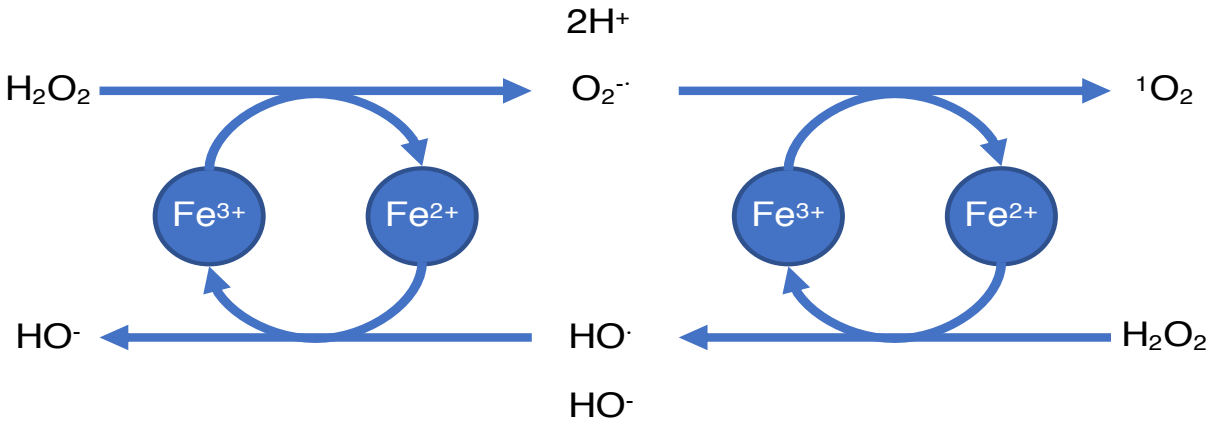

Scheme 1. Postulated singlet oxygen formation mechanism. The overall reaction converts $2H_2O_2$ to $2H_2O + {}^1O_2$.

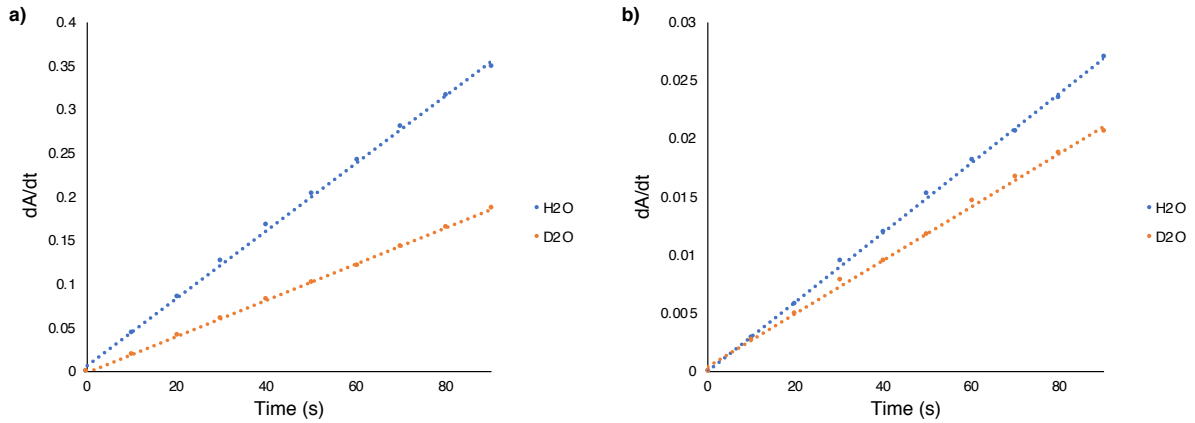

Figure 10. Oxidation of o-phenylenediamine (OPD) in H_2O and D_2O at a) pH 4 and b) pH 7. $[OPD]_0$ = 200 µM; $[FeCl_3]_0$ = 200 µM; $[H_2O_2]$ = 200 mM; [MES] = 1 mM; and T = 25 ºC.

Conclusion

Herein we present evidence supporting the formation of $^1O_2$ during the Fe-catalyzed decomposition of H_2O_2. The reaction rate is unaffected by the presence of Cl^- and is accelerated at low pH values; however, $^1O_2$, rather than $^{\cdot}OH$ radicals, is the main ROS in Fenton reaction at pH 4–7.

Experimental

o-Phenylenediamine, coumarin, XTT sodium salt, sodium chloride, sodium azide, t-butyl alcohol, iron (III) chloride (99.9+%), and 1,3-diphenylisobenzofuran were obtained from Sigma Aldrich (Oakville, ON, Canada). Hydrogen peroxide (30%) and Singlet Oxygen Sensor Green were obtained from Thermo Fisher Scientific (Waltham, MA, USA). Absorbance and fluorescence measurements were performed using a Tecan infinite M1000 Pro plate reader (Zürich, Switzerland). Gas chromatography-mass spectrometry was used to confirm the formation of 1,2-dibenzoylbenzene from 1,3-diphenylisobenzofuran using an Aglient Technologies 6890N gas chromatograph coupled with a 5973 Inert mass spectrum detector (Santa Clara, CA, USA). An NSP-5 Inert capillary column (15 m x 0.25 mm x 0.30 µm, J&K Scientific, Edwardsville, NS, Canada) was used for the separation. The temperature program was initially 55 ºC for 4 min, then ramping at 15 ºC min^{-1} until reaching 130 ºC, then ramping at 20 ºC min^{-1} until reaching 290 ºC and holding for 3 min. Solutions of $FeCl_3$, OPD, and SOSG were prepared fresh immediately before each experiment to prevent sample degradation and all kinetic traces were corrected using suitable blanks. OPD oxidation and XTT reduction were monitored through absorbance at 452 and 470 nm, respectively. Coumarin hydroxylation was monitored via umbelliferone fluorescence (excitation at 325 nm, emission at 452 nm). DPIBF conversion to 1,2-dibenzoylbenzene was monitored by the decrease in DPIBF fluorescence (excitation at 405 nm, emission at 458 nm). SOSG peroxidation was measured through the formation of SOSG-endoperoxide fluorescence (excitation at 504 nm, emission at 525 nm). Notably, SOSG-endoperoxide fluorescence is sensitive to pH and $[Fe^{3+}]$, and suitable blank experiments are required.

References

(1) Fenton, H. J. H. LXXIII.—Oxidation of Tartaric Acid in Presence of Iron. *J. Chem. Soc., Trans.* **1894**, *65* (0), 899–910. https://doi.org/10.1039/CT8946500899.

(2) Prousek, J. Fenton Chemistry in Biology and Medicine. *Pure and Applied Chemistry* **2007**, *79* (12), 2325–2338. https://doi.org/10.1351/pac200779122325.

(3) Haber, F.; Weiss, J. The Catalytic Decomposition of Hydrogen Peroxide by Iron Salts. *Proc. R. Soc. Lond. A* **1934**, *147* (861), 332–351. https://doi.org/10.1098/rspa.1934.0221.

(4) Moffett, J. W.; Zika, R. G. Reaction Kinetics of Hydrogen Peroxide with Copper and Iron in Seawater. *Environ. Sci. Technol.* **1987**, *21* (8), 804–810. https://doi.org/10.1021/es00162a012.

(5) De Laat, J.; Truong Le, G.; Legube, B. A Comparative Study of the Effects of Chloride, Sulfate and Nitrate Ions on the Rates of Decomposition of H2O2 and Organic Compounds by Fe(II)/H2O2 and Fe(III)/H2O2. *Chemosphere* **2004**, *55* (5), 715–723. https://doi.org/10.1016/j.chemosphere.2003.11.021.

(6) Wardman, P. Reduction Potentials of One-Electron Couples Involving Free Radicals in Aqueous Solution. *Journal of Physical and Chemical Reference Data* **1989**, *18* (4), 1637–1755. https://doi.org/10.1063/1.555843.

(7) Liao, C.; Kang, S.; Wu, F. Hydroxyl Radical Scavenging Role of Chloride and Bicarbonate Ions in the H2O2/UV Process. *Chemosphere* **2001**, *44* (5), 1193–1200. https://doi.org/10.1016/s0045-6535(00)00278-2.

(8) Bray, W. C.; Gorin, M. H. FERRYL ION, A COMPOUND OF TETRAVALENT IRON. *J. Am. Chem. Soc.* **1932**, *54* (5), 2124–2125. https://doi.org/10.1021/ja01344a505.

(9) Kim, S.; Fujitsuka, M.; Majima, T. Photochemistry of Singlet Oxygen Sensor Green. *J. Phys. Chem. B* **2013**, *117* (45), 13985–13992. https://doi.org/10.1021/jp406638g.

(10) Carloni, P.; Damiani, E.; Greci, L.; Stipa, P.; Tanfani, F.; Tartaglini, E.; Wozniak, M. On the Use of 1,3-Diphenylisobenzofuran (DPBF). Reactions with Carbon and Oxygen Centered Radicals in Model and Natural Systems. *Research on Chemical Intermediates* **1993**, *19* (5), 395–405. https://doi.org/10.1163/156856793X00181.

(11) Krieg, M. Determination of Singlet Oxygen Quantum Yields with 1,3-Diphenylisobenzofuran in Model Membrane Systems. *Journal of Biochemical and Biophysical Methods* **1993**, *27* (2), 143–149. https://doi.org/10.1016/0165-022X(93)90058-V.

(12) Bancirova, M. Sodium Azide as a Specific Quencher of Singlet Oxygen during Chemiluminescent Detection by Luminol and Cypridina Luciferin Analogues. *Luminescence* **2011**, *26* (6), 685–688. https://doi.org/10.1002/bio.1296.

(13) Li, M. Y.; Cline, C. S.; Koker, E. B.; Carmichael, H. H.; Chignell, C. F.; Bilski, P. Quenching of Singlet Molecular Oxygen (1O2) by Azide Anion in Solvent Mixtures. *Photochem. Photobiol.* **2001**, *74* (6), 760. https://doi.org/doi.org/10.1562/0031-8655(2001)074<0760:QOSMOO>2.0.CO;2.

(14) Staehelin, J.; Hoigne, J. Decomposition of Ozone in Water in the Presence of Organic Solutes Acting as Promoters and Inhibitors of Radical Chain Reactions. *Environ. Sci. Technol.* **1985**, *19* (12), 1206–1213. https://doi.org/10.1021/es00142a012.

(15) Louit, G.; Foley, S.; Cabillic, J.; Coffigny, H.; Taran, F.; Valleix, A.; Renault, J. P.; Pin, S. The Reaction of Coumarin with the OH Radical Revisited: Hydroxylation Product Analysis Determined by Fluorescence and Chromatography. *Radiation Physics and Chemistry* **2005**, *72* (2), 119–124. https://doi.org/10.1016/j.radphyschem.2004.09.007.
(16) Zhang, J.; Nosaka, Y. Quantitative Detection of OH Radicals for Investigating the Reaction Mechanism of Various Visible-Light TiO2 Photocatalysts in Aqueous Suspension. *J. Phys. Chem. C* **2013**, *117* (3), 1383–1391. https://doi.org/10.1021/jp3105166.
(17) Pestovsky, O.; Stoian, S.; Bominaar, E. L.; Shan, X.; Münck, E.; Que Jr., L.; Bakac, A. Aqueous FeIV=O: Spectroscopic Identification and Oxo-Group Exchange. *Angewandte Chemie International Edition* **2005**, *44* (42), 6871–6874. https://doi.org/10.1002/anie.200502686.
(18) Wiegand, H. L.; Orths, C. T.; Kerpen, K.; Lutze, H. V.; Schmidt, T. C. Investigation of the Iron–Peroxo Complex in the Fenton Reaction: Kinetic Indication, Decay Kinetics, and Hydroxyl Radical Yields. *Environ. Sci. Technol.* **2017**, *51* (24), 14321–14329. https://doi.org/10.1021/acs.est.7b03706.
(19) Corey, E. J.; Mehrotra, M. M.; Khan, A. U. Antiarthritic Gold Compounds Effectively Quench Electronically Excited Singlet Oxygen. *Science* **1987**, *236* (4797), 68–69. https://doi.org/10.1126/science.3563489.
(20) Khan, A. U. Near Infrared Emission of Singlet Oxygen Generated in the Dark. *J. Biolumin. Chemilumin.* **1989**, *4* (1), 200–207. https://doi.org/10.1002/bio.1170040129.
(21) Able, A.; Guest, D.; Sutherland, M. Use of a New Tetrazolium-Based Assay to Study the Production of Superoxide Radicals by Tobacco Cell Cultures Challenged with Avirulent Zoospores of Phytophthora Parasitica Var Nicotianae. *Plant physiology* **1998**, *117* (2), 491–499.
(22) Armstorng, D. A.; Huie, R. E.; Lymar, S.; Koppenol, W. H.; Merényi, G.; Neta, P.; Stanbury, D. M. Standard Electrode Potentials Involving Radicals in Aqueous Solution: Inorganic Radicals. *Bioinorg. React. Mech.* **2014**, *9* (1–4), 59. https://doi.org/doi:10.1515/irm-2013-0005.
(23) Bregnhøj, M.; Westberg, M.; Jensen, F.; Ogilby, P. R. Solvent-Dependent Singlet Oxygen Lifetimes: Temperature Effects Implicate Tunneling and Charge-Transfer Interactions. *Phys. Chem. Chem. Phys.* **2016**, *18* (33), 22946–22961. https://doi.org/10.1039/C6CP01635A.